

# Effects of head wear performance with respect to the lubricant thickness on hard disk media for ultra-thin lubricants

Ichiro Ota<sup>1</sup> · Hiroyuki Tomita<sup>1</sup> · Katsumi Murofushi<sup>1</sup>

Received: 23 September 2015 / Accepted: 1 February 2016 / Published online: 18 February 2016  
© Springer-Verlag Berlin Heidelberg 2016

**Abstract** Magnetic head wear performance was studied using various thicknesses of D-4OH lubricant that covers hard disk media. The characteristic head wear behavior to over-push the dynamic flying height power differed for each lubricant thickness. The difference in the behavior was highly dependent on the media friction coefficient. The surface free energy also varied as a function of the lubricant thickness. According to the lubricant coverage analysis, we found that the head wear behavior and the friction were dependent on the lubricant coverage change as a function of the lubricant thickness. Furthermore, the molecular dynamics method was applied to investigate the lubricant molecular distribution; the coverage changed with the lubricant thickness similar to that in the experiment. Finally, a head–disk interface mechanism under an over-pushed state was discussed, and meniscus bridge formation was suggested to have occurred at touchdown power for each lubricant thickness.

## 1 Introduction

Various studies to develop novel technology have been conducted to meet the continuous demand of increasing the areal density of hard disk (HD) drives. Reducing the distance between the transducer of the magnetic head and magnetic layer of HD media (magnetic spacing) is essential to enhance the magnetic recording signal/noise ratio.

Dynamic flying height (DFH) control technology was developed in the mid 2000s to stabilize the space from the transducer of a magnetic head to the magnetic media (head media spacing, HMS). The DFH technology can help reduce the HMS from 10 to 3 nm. In recent times, the HMS has become less than 1 nm. Further, HMS reduction is expected to increase the recording density in the future. Intermittent contact occurs at the sub-1-nm HMS region. Li et al. showed that the head slider starts to intermittently contact during a flying test at a 0.5-nm clearance (Matthes et al. 2013). Pseudo-contact recoding could be realized in the future to obtain a higher areal recording density. In addition, the thickness of the carbon protective layer and lubricant is reduced. The lubricant thickness should be less than 1 nm. On the other hand, these reductions must influence the wear side; hence, maintaining reliable performance has become increasingly important. The wear performance of magnetic heads has recently become an important requirement in ultra-thin lubricants among the various reliability requirements. Free lubricants and lubricant viscosity could be key factors in minimizing head wear. Matthes et al. indicated that head wear may be correlated with the type of lubricant and its bonded ratio. They also indicated that free lubricant could help resist head wear (Li et al. 2009). They also focused on the slider design because it is considered a key factor. Juang et al. studied head wear via over-pushed stress tests using three types of heads with different DFH protrusion profiles. This process was done to compare the flyability and durability of the heads using scanning electron microscope (SEM) images (Juang et al. 2011). On the other hand, Kobayashi et al. studied head wear under constant over-push for various lubricants (molecular weight and lubricant type) and explained the relationship between the head wear and lubricant coverage (Kobayashi et al. 2014).

✉ Ichiro Ota  
ota.ichiro.xhrcc@showadenko.com

<sup>1</sup> Institute for Polymers and Chemicals, Business Development Center, Showa Denko K. K., 5-1 Yawata Kaigan Dori, 290-0067 Ichihara, Chiba, Japan

Tani et al. used the molecular dynamics (MD) method to investigate the lubricants on an HD surface to study the molecular conformation of various types of lubricants. They found that each lubricant has its own conformation on the HD media (Tani et al 2009).

Against this background, we conducted head wear tests as a function of the lubricant thickness. A change in the head wear rate was observed as the DFH over-pushed stress was gradually increased. Through friction, surface free energy, and lubricant coverage measurement, a hypothesis on the mechanism of the wear rate change was proposed. We aim to clarify the wear and lubrication mode through a head wear study in the over-pushed state. We also aim to study the relationship of wear with the lubricant coverage of the HD media.

## 2 Experimental and results

### 2.1 Sample disks and lubricants

The media used in this study were 2.5-in. glass substrate disks with a nitrogenized diamond-like-carbon overcoat (2-nm thick). The media had perpendicular magnetic recording layers, and the average surface roughness ( $R_a$ ) of the disks was approximately 0.20 nm, as measured by atomic force microscopy. The disks were coated with lubricant films with various thicknesses (8.5, 14, and 18 Å) via a dip-coating process under ambient conditions and a thermal treatment process at 450 K. The lubricant we used was D-4OH (Moresco), as shown in Fig. 1. The molecular weight of D-4OH is 2000. The thickness of the lubricant film was measured using Fourier transform infrared spectroscopy (FTIR), calibrated using an X-ray reflectometer. To prevent the free-lubricant effect (bonded-ratio effect), we employed an identical bonded ratio of approximately 75 % for all three conditions.

### 2.2 Magnetic head wear experiments

To estimate the reliability risk in an ultra-thin lubricant, magnetic head wear tests were performed for three lubricant thicknesses (8.5, 14, and 18 Å) of the magnetic media. A magnetic head and the magnetic media were set up on a spin stand, as shown in Fig. 2. The magnetic head constantly flies on the media at a radius of 20 mm under ambient conditions (25 °C and 40 % RH). The rotational speed

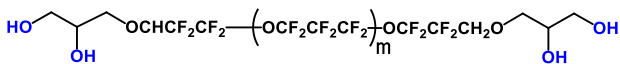


**Fig. 1** Chemical structure of D4OH

of the media was 5400 rpm. The touchdown of the DFH protrusion on the media was detected using an acoustic emission (AE) detector. Its power is defined as touchdown

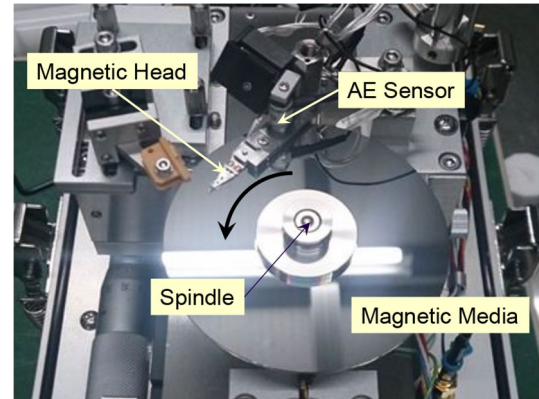


**Fig. 2** Mechanical setting of head wear test

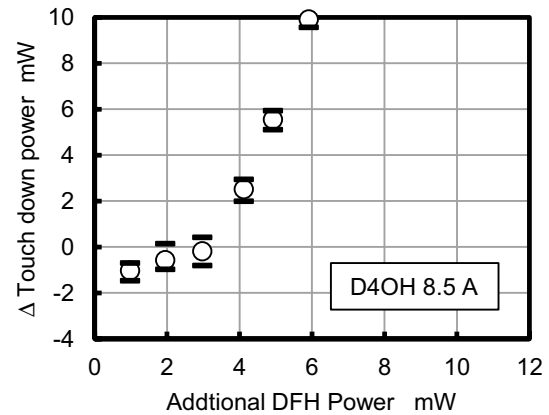


**Fig. 3**  $\Delta$ Touchdown power trend in D4OH 8.5 Å as a function of over-pushed DFH power

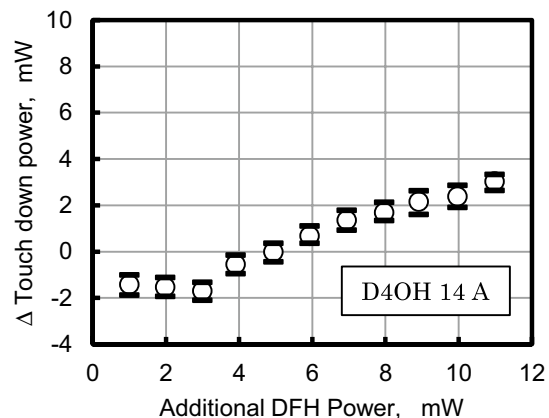


**Fig. 4**  $\Delta$ Touchdown power trend in D4OH 14 Å as a function of over-pushing DFH power

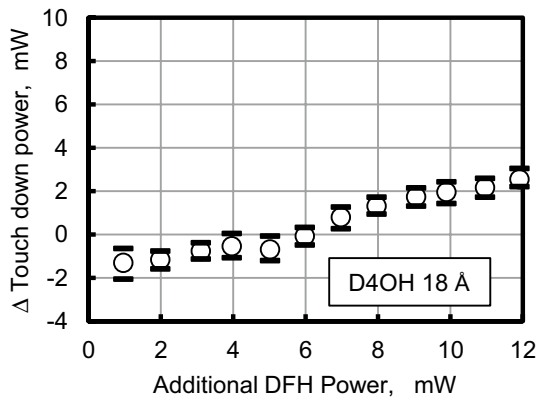


**Fig. 5**  $\Delta$ Touchdown power trend in D4OH 18 Å as a function of over-pushing DFH power

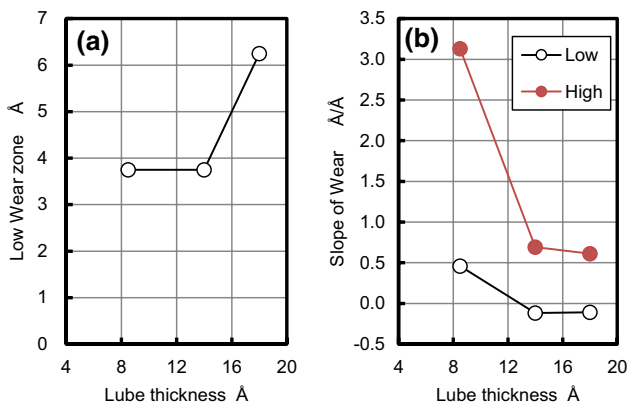


**Fig. 6** Range of low wear rate (a), and slope of low wear rate (b), and slope of high wear rate as a function of lube thickness obtained from Figs. 3, 4, and 5

power. We selected a highly sensitive AE sensor. A stress test was conducted for 100 s by applying an additional 1–12 mW DFH power to over-push the protrusion. A different radius ( $r = 21$  mm) was used in the over-pushing because the media surface could be flattened after the over-pushed head–disk interface (HDI) contact. Thereafter, the touchdown power was measured one more time. The difference in the touchdown power before and after the stress test is defined as  $\Delta$ touchdown power, which is regarded as an index of head wear.

Magnetic head wear tests as a function of the additional DFH power from the touchdown power were performed, as shown in Figs. 3, 4, and 5. We can observe that two different wear zones appeared with the additional DFH power in the over-pushed state. In the 8.5-Å case (Fig. 3), the wear slowly increased (wear rate: 0.46 Å/Å) up to +3 mW, after which it sharply increased (wear rate: 3.1 Å/Å). Here, The denominator (Å) is converted from the efficiency of DFH to input power. A power of 8 mW is necessary to change a 1 nm DFH

protrusion. In the 14-Å case, the wear did not increase up to +3 mW, after which it started to increase. However, the wear rate was apparently smaller than that in the 8.5-Å case (wear rate: 0.69 Å/Å). In the 18-Å case, no wear was observed up to +5 mW, after which the wear started to increase in a manner similar to that in the 14-Å case. In addition, the wear rate was 0.61 Å/Å, which was similar to that in the 14-Å case. Figure 6 shows the relationship between the wear rate and lubricant thickness; some characteristics are observed as follows: the range of the lower wear rate was constant up to 14 Å. The wear rate was almost constant beyond 14 Å. The lower wear rate in the 8.5-Å case was similar to the higher wear rate of the 14- and 18-Å cases. The physical wear in all cases was checked and confirmed by SEM images; thus, we observed a pole tip portion of a magnetic head.

We performed a head vibration analysis using fast Fourier transform (FFT). A lower frequency (~100 kHz) was observed at the touchdown point and continued. A higher frequency (~330 kHz) was observed at a few milliwatt over-push after touchdown. A higher frequency vibration could be simultaneously observed as the wear rate changes.

### 2.3 Media friction coefficient measurement

To study the different wear tendencies as a function of lubricant thickness, the media friction was measured as a function of the lubricant thickness. A friction tester was prepared using a pin-on-disk type suspension that had an alumina ball (diameter: 4 mm) in contact with the media. The rotational speed was 100 rpm, and the measurement radius was 20 mm under ambient conditions (25 °C and 40 % RH).

Figure 7 shows that the friction coefficient started from 0.6 and remained approximately at this value up to 5 Å, after which the coefficient decreased with the increase in the lubricant thickness. The friction coefficient saturated at 0.24 at a thickness of approximately 15 Å. The friction curve was similar to the Stribeck curve obtained using mixed lubrication.

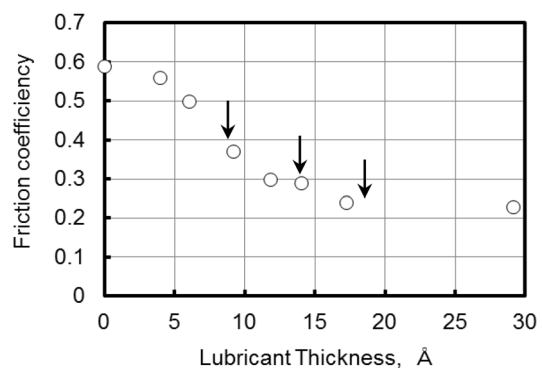


**Fig. 7** Friction coefficient as a function of lubricant thickness

### 2.4 Surface free-energy measurement

The surface free energy of the media was measured using the Lifshitz–van der Waals/Lewis acid–base (LW/AB) theory (van Oss 2002). A polar component ( $\gamma^{AB}$ ) and a Van der Waals component ( $\gamma^{LW}$ ) were obtained from the LW/AB theory. The formulas are shown as follows:

$$\begin{aligned} \gamma &= \gamma^{LW} + \gamma^{AB} \quad \text{here,} \\ \gamma^{AB} &= 2\sqrt{\gamma^+ \gamma^-} \end{aligned} \quad (1)$$

Three test liquids with known surface energy parameters are required to determine the three unknown parameters ( $\gamma_s^{LW}$ ,  $\gamma_s^+$ ,  $\gamma_s^-$ ) by solving the following equations:

$$\begin{aligned} \gamma_{Li}(1 + \cos \theta_i) &= 2 \left( \sqrt{\gamma_s^{LW} \gamma_{Li}^{LW}} + \sqrt{\gamma_s^+ \gamma_{Li}^-} + \sqrt{\gamma_s^- \gamma_{Li}^+} \right) \\ i &= 1, 2, 3 \end{aligned} \quad (2)$$

Here,  $\theta_i$  is the contact angle, and  $i$  represents the test liquids. The three test liquids we used were water ( $\gamma^{LW} = 21.8 \text{ mJ/m}^2$ ,  $\gamma^{AB} = 51.0 \text{ mJ/m}^2$ , and  $\gamma^+ = \gamma^- = 25.5 \text{ mJ/m}^2$ ), 1-bromonaphthalene ( $\gamma^{LW} = 43.5 \text{ mJ/m}^2$  and  $\gamma^{AB} = \gamma^+ = \gamma^- = 25.5 \text{ mJ/m}^2$ ), and glycerin ( $\gamma^{LW} = 34.0 \text{ mJ/m}^2$ ,  $\gamma^{AB} = 29.9 \text{ mJ/m}^2$ ,  $\gamma^+ = 3.9 \text{ mJ/m}^2$ , and  $\gamma^- = 57.4 \text{ mJ/m}^2$ ).

The lubricant coverage is calculated using  $\gamma^{LW}$  and the equation presented by Kobayashi et al. (2014).

$$\begin{aligned} \gamma_s^{LW}(h) &= \gamma_{bulk}^{LW} + \frac{A^*}{24\pi(d_0 + h)} \\ \gamma_s^{LW}(h) &= \alpha(h)\gamma_{mono}^{LW} + (1 - \alpha)\gamma_s^{LW}(0) \\ \alpha(h) &= \frac{\gamma_s^{LW}(0) - \gamma_s^{LW}(h)}{\gamma_s^{LW}(0) - \gamma_{mono}^{LW}} \end{aligned}$$

$\gamma^{AB}$  and  $\gamma^{LW}$  exhibited a simple decrease. Figure 8 shows  $\gamma^{LW}$  as a function of the lubricant thickness.  $\gamma^{LW}$  of the unlubricated media was  $41 \text{ mJ/m}^2$ , and it decreased with the increase in the lubricant thickness. The value saturated at  $15 \text{ mJ/m}^2$  at  $14 \text{ \AA}$ . The lubricant coverage was evaluated as a function of the lubricant thickness, as shown in Fig. 9. The coverage increased with the lubricant thickness by approximately 80 % at  $8 \text{ \AA}$ , 96.7 % at  $14 \text{ \AA}$ , and 97.7 % at  $18 \text{ \AA}$ .

Figure 10 shows the relationship between the lubricant coverage and friction coefficient. A good correlation could be observed from the figure.

### 2.5 MD simulation

We attempted to investigate the adhesion behavior of the lubricant using the MD method. A graphite continuous

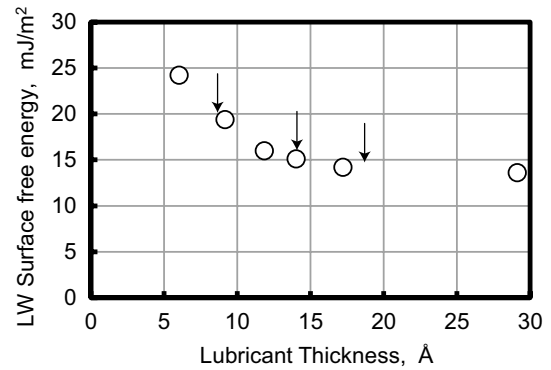


Fig. 8 Dependence of  $\gamma^{LW}$  as a function of lubricant thickness

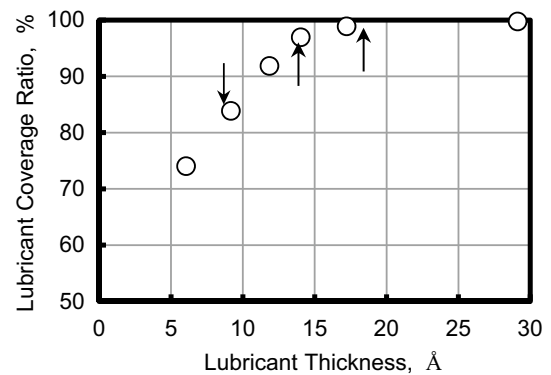


Fig. 9 Lubricant coverage as a function of lubricant thickness

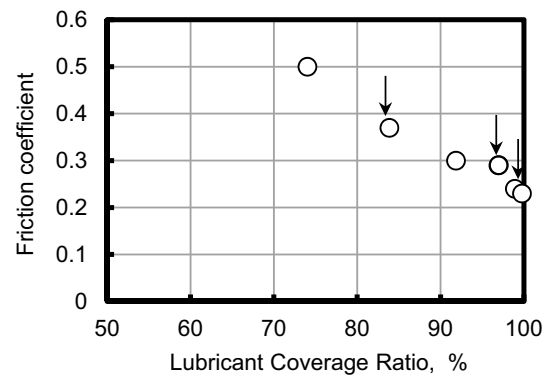
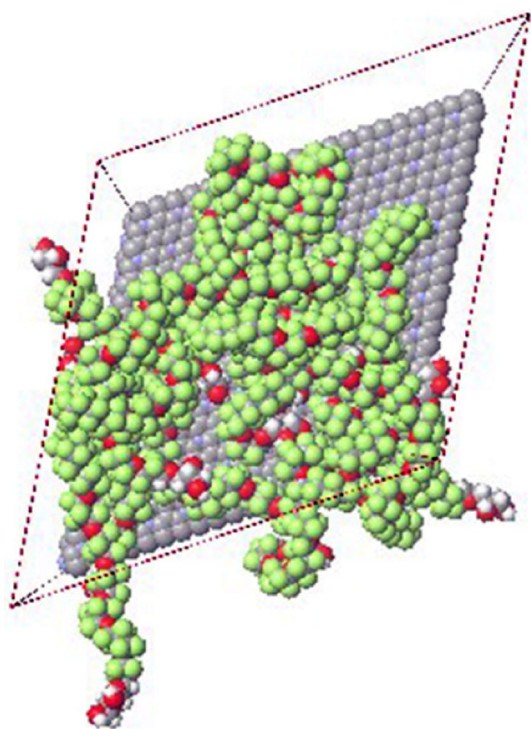


Fig. 10 Friction coefficient as a function of lubricant coverage ratio

layer where 13 % of nitrogen atoms were exchanged from carbon atoms was used as the substrate surface of a carbon protective layer. The lubricant molecules were deposited on the carbon layer in an MD cell. A periodic boundary condition was applied for the MD cell. The lubricant molecules were initially processed at 450 K and at 300 K thereafter. The 450-K temperature was used in the thermal curing process of the HD media, and the 300-K temperature was



**Fig. 11** Lubricant (10-Å thick) distribution image on the carbon surface of HD media

used for cooling. Molecule conformation was optimized during the process to minimize the potential energy of the molecules. The thermal curing and cooling process times were set to 2 and 3 ns, respectively, due to the limitations in the calculation. The partial charges of the lubricant molecules and the carbon protective layer were determined by an ab initio molecular orbital method.

After the treatment process, the lubricant thickness and lubricant coverage were calculated. Defining the lubricant thickness is interesting because the MD method only shows the coordinates of the lubricant molecular atoms and does not provide the actual thickness of the lubricant. To calculate the lubricant thickness from the coordinates of the lubricant, the MD cell was divided into 3-Å cubes in the area above the carbon layer where the lubricant was distributed. The 3-Å cube was selected because the Van der Waals diameter of fluorine is 1.47 Å, and fluorine occupies approximately a 3-Å cube. In the next step, cubes that include carbon, oxygen, and fluorine atoms were collected, and the collected cubes were defined as a lubricant layer. Because we measured the lubricant thickness by FTIR, which has a spot size of few millimeters, the average height of the lubricant layer was considered as the lubricant thickness. A typical MD result is shown in Fig. 11.

Figure 12 shows the comparison of the lubricant coverage calculated by the MD method with actual dependence of the coverage as a function of the lubricant thickness.

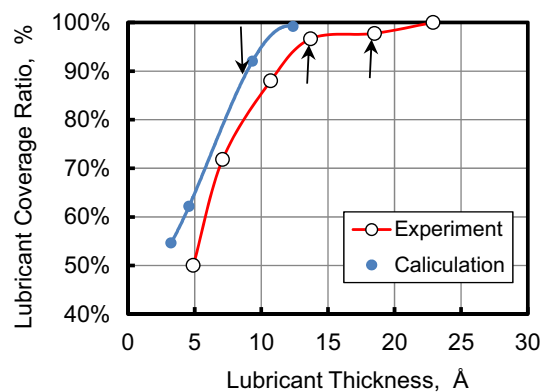


**Fig. 12** Comparison of lubricant coverage calculated by MD with actual coverage as a function of lubricant thickness

According to the MD lubricant thickness method, the lubricant coverage calculated by the MD method could be correlated with the lubricant coverage obtained from the experiment. However, it was approximately 5–15 % higher. Considering the roughness of the media surface is necessary because uncovered areas could appear on peaks of the surface to decrease the coverage.

### 3 Discussion

The HDI mechanism in the over-pushed state can be explained as follows. In the lower wear zone, the resonance frequency is similar to the touchdown frequency, according to the analysis. In other words, the head pole tip can come into contact with the media lubricant. Until the media surface is fully covered, friction can change with the increase in coverage. Therefore, the wear rate varies with the coverage.

On the other hand, in the higher wear zone, the head pole tip can come into contact with the carbon overcoat, and because of the solid–solid contact, the head vibration frequency could be higher (~330 kHz). The wear rate is higher if the coverage is lower. However, once the media surface is fully covered, the wear rate becomes constant.

For the wear rate shown in Fig. 6, the lubricant coverage can explain the wear rate. For a lower coverage, friction is higher due to the solid contact of the head slider with the carbon overcoat, which increases the wear rate. The friction and the wear rate could decrease when the coverage increase. If the lubricant thickness is beyond the monolayer thickness, the friction and wear rate could be constant because the carbon overcoat is fully covered with lubricant.

Tani reported that the PFPE lubricant could cover from a valley on the HD media surface for lubricant coverage of less than 100 % (Tani 1999). From his study, we could consider that many topological protrusions are exposed under

the condition that the coverage does not reach 100 % ( $R_a$  is  $\sim 0.2$  nm,  $R_p$  is  $\sim 0.6$  nm, and  $R_v$  is  $\sim 0.6$  nm in the case of the current perpendicular magnetic recording media). If the head pole starts to touch the peak of the protrusions, head wear occurs due to the initial contact between the head pole and the carbon surface of the media. At this instant, the frequency of the head vibration is higher ( $\sim 300$  kHz). However, previous results indicated that a soft contact area always appears for each thickness, which implies that the head starts from the contact with the lubricant, which is in contrast to the hypothesis that stated that the head starts from the contact with carbon.

Here, the touchdown power was measured and shown in Fig. 13 as a function of the lubricant thickness. If the touchdown power depends on the lubricant coverage, it should be constant because the head pole should always start from the initial contact with the surface protrusions. However, from the results shown in Fig. 13, we found that the touchdown power simply decreased as the lubricant thickness increased even under a monolayer thickness (less than  $15 \text{ \AA}$ ). The experimental result is in contrast to the hypothesis that stated that the head starts from the contact with the carbon.

From these two contradictions to the hypothesis, we can see that some amount of lubricant always exists between the head pole tip and the media, resulting in meniscus bridge formation even if the lubricant thickness does not become identical to the monolayer thickness.

Figure 14 shows schematic images of the HDI for the three lubricant thicknesses. Even if the lubricant thickness does not help attain full coverage, head wear does not occur, and meniscus bridges are formed. A  $3.6\text{-\AA}$  meniscus space should exist in the  $8.5\text{-\AA}$  case, and  $14\text{-}$  and  $7.2\text{-\AA}$  meniscus spaces should exist in the  $18\text{-\AA}$  case. The low wear rate in the  $8.5\text{-\AA}$  case is similar to the high wear rate of the fully covered media because the contact point of the HDI is fully covered with lubricant as the meniscus bridge and friction are constant in the nanoscale area.

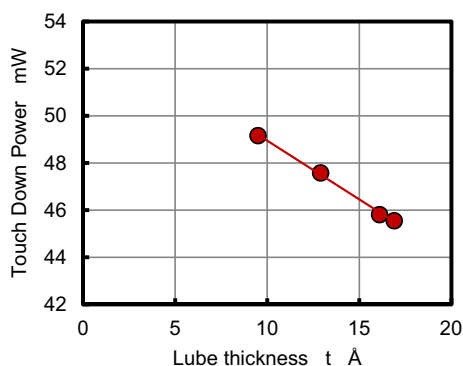


**Fig. 13** Touchdown power as a function of lubricant thickness

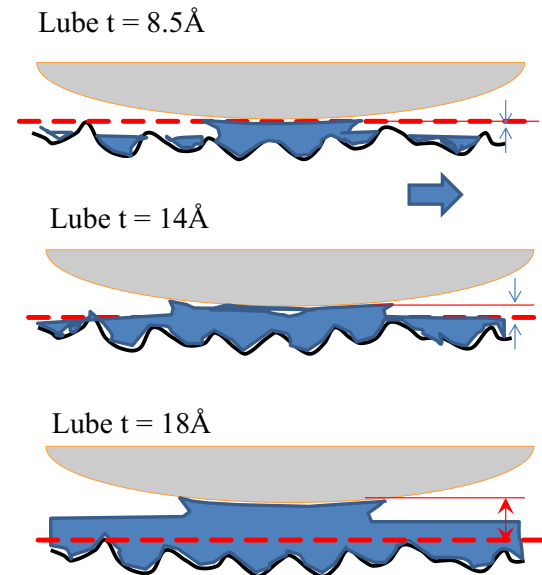


**Fig. 14** Schematic images of the HDI for the three lubricant thicknesses

## 4 Conclusion

We have studied magnetic head wear performance as a function of lubricant thickness when the DFH over-pushed stress gradually increased. The results are as follows:

1. Lower and higher wear zones were observed in all three thicknesses. They have specific behavior from the viewpoint of the wear rate.
2. The friction coefficient was correlated with the lubricant coverage. Both the lower and higher wear zones were also correlated with the lubricant coverage.
3. According to the FFT analysis, the lower wear zone can be understood as mixed lubrication and the higher wear zone can be considered as boundary lubrication in the macroscopic scale.
4. The MD simulation results well fitted with the actual lubricant coverage as a function of the lubricant thickness. We have shown that lubricant conformation and the number determine the coverage.
5. Considering surface topology, even in areas where the lubricant coverage was less than 100 %, a meniscus was formed as a lower wear zone, although it was believed that boundary lubrication is dominant in the area.

## References

- Juang JY, Forrest J, Huang FY (2011) Magnetic head protrusion profiles and wear pattern of thermal flying-height control sliders with different heater designs. *IEEE Trans Magn* 47:3437–3440

- Kobayashi N, Tani H, Shinji T, Koganezawa S, Tagawa N (2014) Slider wear on disks lubricated by ultra-thin perfluoropolyether lubricants with different molecular weights. *Tribol Lett* 53:43–49
- Li N, Zheng L, Meng Y, Bogy DB (2009) Experimental study of head-disk interface flyability and durability at sub-1-nm clearance. *IEEE Trans Magn* 45:3624–3627
- Matthes L, Brunner R, Knigge B, Talke FE (2013) Investigation of head burnishing of thermal flying height control sliders. CD-ROM of ISPS2013, No.2013-2909. Santa Clara, CA, USA. 24, 25 June 2013
- Tani H (1999) Observation of PFPE lubricant film on magnetic disk surface by atomic force microscopy. *IEEE Trans Magn* 35(5):2397–2399
- Tani H, Sakamoto K, Tagawa N (2009) Conformation of ultra-thin PFPE lubricant with different structure on magnetic disks - direct observation and MD simulation -. In: *Proceeding of Asia-Pacific Magnetic Recording Conference 2009, APMRC 2009, CB-2*
- van Oss CJ (2002) Use of the combined Lifshitz–van der Waals and Lewis acid–base approaches in determining the apolar and polar contributions to surface and interfacial tensions and free energies. *J Adhesion Sci Technol* 16(6):669–677